Journal of Structural Geology 30 (2008) 1405–1411

Contents lists available at ScienceDirect

Journal of Structural Geology

journal homepage: www.elsevier.com/locate/jsg

Dependence of displacement–length scaling relations for fractures and deformation bands on the volumetric changes across them

Richard A. Schultz [a,*], Roger Soliva [b], Haakon Fossen [c,d], Chris H. Okubo [e], Donald M. Reeves [f]

[a] Geomechanics-Rock Fracture Group, Department of Geological Sciences and Engineering/172, University of Nevada, Reno, NV 89557-0138, USA
[b] Université Montpellier II, Laboratoire Géosciences Montpellier, 34000 Montpellier, France
[c] Centre for Integrated Petroleum Research, University of Bergen, Allégaten 41, N-5007 Bergen, Norway
[d] Department of Geoscience, University of Bergen, Allégaten 41, N-5007 Bergen, Norway
[e] U.S. Geological Survey, 2255 North Gemini Drive, Flagstaff, AZ 86001, USA
[f] Desert Research Institute, 2215 Raggio Parkway, Reno, NV 89512, USA

ARTICLE INFO

Article history:
Received 8 January 2008
Received in revised form 8 July 2008
Accepted 1 August 2008
Available online 9 August 2008

Keywords:
Scaling
Faulting
Deformation bands
Compaction bands

ABSTRACT

Displacement–length data from faults, joints, veins, igneous dikes, shear deformation bands, and compaction bands define two groups. The first group, having a power-law scaling relation with a slope of $n = 1$ and therefore a linear dependence of maximum displacement and discontinuity length ($D_{max} = \gamma L$), comprises faults and shear (non-compactional or non-dilational) deformation bands. These shearing-mode structures, having shearing strains that predominate over volumetric strains across them, grow under conditions of constant driving stress, with the magnitude of near-tip stress on the same order as the rock's yield strength in shear. The second group, having a power-law scaling relation with a slope of $n = 0.5$ and therefore a dependence of maximum displacement on the square root of discontinuity length ($D_{max} = \alpha L^{0.5}$), comprises joints, veins, igneous dikes, cataclastic deformation bands, and compaction bands. These opening- and closing-mode structures grow under conditions of constant fracture toughness, implying significant amplification of near-tip stress within a zone of small-scale yielding at the discontinuity tip. Volumetric changes accommodated by grain fragmentation, and thus control of propagation by the rock's fracture toughness, are associated with scaling of predominantly dilational and compactional structures with an exponent of $n = 0.5$.

1. Introduction

Displacement–length (D–L) scaling relations for faults and other common geologic structures provide a window into the mechanics of brittle strain localization in compact and porous rocks. D–L scaling relations of faults are well understood, yielding information on the mechanics of localized shear deformation. Maximum displacement D_{max} and horizontal fault length L are related by $D_{max} = \gamma L^n$, with n for fault populations generally being in the range of 1.0 (e.g. Cowie and Scholz, 1992a; Clark and Cox, 1996; Scholz, 2002; Xu et al., 2005). Neglecting the influence of short-range mechanical interaction and other effects, fault populations therefore generally define a linear dependence of maximum displacement and discontinuity length ($D_{max} = \gamma L$). In contrast, the scaling of dilatant structures has been less clear. Early work by Vermilye and Scholz (1995) suggested that veins and igneous dikes scale as $n = 1$, similar to faults. However, re-analysis by Olson (2003) showed that those veins and dikes scale as $n = 0.5$ ($D_{max} = \alpha L^{0.5}$), consistent with growth under conditions of constant rock properties (i.e. the opening-mode fracture toughness, K_{Ic}) instead of constant driving stress (that is a function of friction and normal stress, as in the case of faults; e.g. Scholz, 2002, p. 116). With displacement–length data now available for joints and three varieties of deformation bands including compaction bands, a more comprehensive investigation of the scaling relations for all three kinematic types of structures (opening, shearing, and closing) and both discontinuity classes (sharp vs. tabular; Aydin et al., 2006; Schultz and Fossen, 2008) is now possible.

In this paper we compile and present displacement–length data for the various types of geologic structural discontinuities, including faults, joints, veins, igneous dikes, shear deformation bands, and compaction bands. We then show how the slopes and intercepts of the associated scaling laws contain physical information on the mechanics and propagation of these common structures.

2. Data compilation

Measurements of displacement–length data from the literature for the principal types of geologic structural discontinuities

* Corresponding author.
E-mail address: schultz@mines.unr.edu (R.A. Schultz).

0191-8141/$ – see front matter © 2008 Elsevier Ltd. All rights reserved.
doi:10.1016/j.jsg.2008.08.001

(Schultz and Fossen, 2008) are presented in Figs. 1–4. The data shown exhibit an intrinsic scatter due to several factors (e.g. Schultz, 1999) including mechanical interaction, three-dimensional shape (Willemse et al., 1996; Schultz and Fossen, 2002), and where along the structure's surface the displacement was measured (e.g. Xu et al., 2005), but following standard practice (e.g. Clark and Cox, 1996) the data are compared collectively by calculating or using values of maximum displacement. In all diagrams the axis ranges and labels are consistent, facilitating comparisons between the different types of structures.

The data for faults are compiled and presented in Fig. 1. Fault populations are seen in the figure to scale linearly in displacement and length (Cowie and Scholz, 1992a; Xu et al., 2005; dotted lines in Fig. 2), with the proportionality γ ranging between 10^{-1} and 10^{-3} for the full data set and with smaller ranges of γ for individual fault populations within the same lithology and tectonic environment (Clark and Cox, 1996; Schultz et al., 2006).

Six data sets for joints, veins, and igneous dikes are shown in Fig. 2, with the three new data sets not investigated by Olson (2003) shown with regression lines in bold. These new measurements double the number of dike data sets, increase the number of data sets for veins, and add a data set for joints, which were previously not represented, to the database compiled and shown in the figure. As evident in Fig. 2, opening-mode structures plot with distributions more consistent with $L^{0.5}$ (dashed lines in Fig. 2) than with linear scaling (dotted lines in Fig. 2), implying a different physical control on their scaling relations than is the case for faults.

Several data sets are now available for deformation bands (Fossen et al., 2007). The cataclastic compactional shear deformation bands measured by Fossen and Hesthammer (1997) and a second data set for these structures reported by Wibberley et al. (2000) scale approximately as $n = 0.5$ (Fig. 3, filled triangles). Two data sets for disaggregation deformation bands for which volumetric strains appear to be negligible, compiled by Fossen et al. (2007), and one for slip surfaces in low-porosity sandstone and described in the Appendix, exhibit steeper slopes close to $n = 1.0$ (Fig. 3).

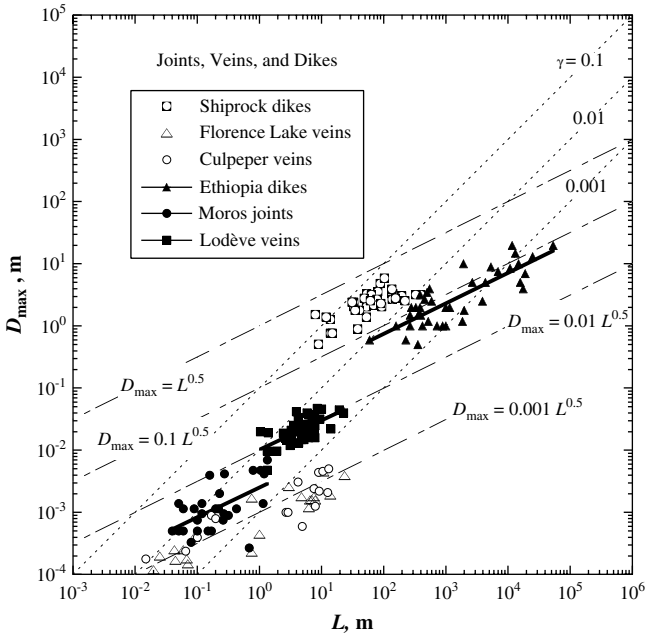

Fig. 2. Compilation of joints, veins, and dikes; see Olson (2003), the Appendix, and the text for sources of data and discussion. Lines of constant slope are shown: $n = 1$, dotted, as in Fig. 1; $n = 0.5$, dashed. Heavy lines show power-law fits to the data sets not analyzed by Olson (2003). Ethiopia dikes: $D_{max} = 0.078L^{0.49}$, $r^2 = 0.66$; Moros' joints: $D_{max} = 0.0025L^{0.48}$, $r^2 = 0.45$; Lodève sparitic sinuous veins: $D_{max} = 0.01L^{0.47}$, $r^2 = 0.41$.

The final plot shows the scaling relations for compaction bands in sandstone, represented by data from the two currently known localities (Mollema and Antonellini, 1996; Sternlof et al., 2005; Schultz, in press). Compaction bands are a variety of deformation band that accommodates contractional normal strain with little or no shear strain across the band (Mollema and Antonellini, 1996; Sternlof et al., 2005; Schultz and Siddharthan, 2005; Aydin et al., 2006; Holcomb et al., 2007; Schultz and Fossen, 2008). The data

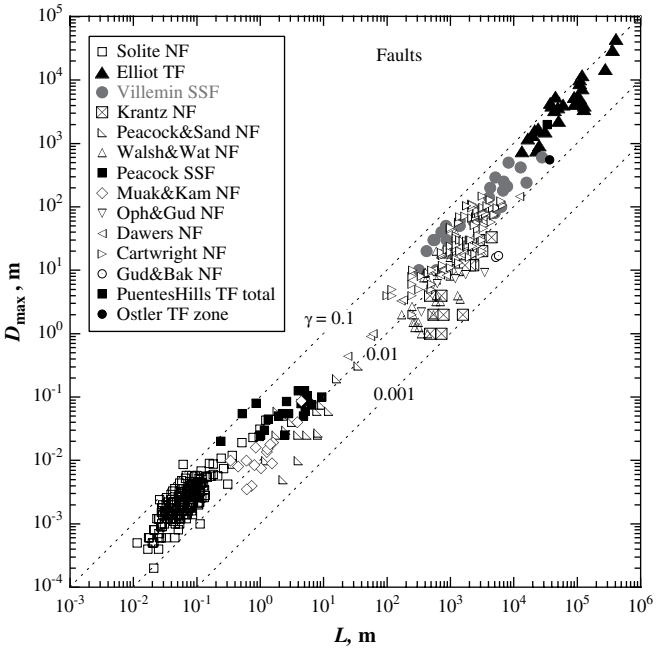

Fig. 1. Compilation of faults; see Cowie and Scholz (1992a), Schlische et al. (1996), and Schultz et al. (2006) for sources of data and discussion. Normal faults (NF), open symbols; strike-slip faults (SSF), gray symbols; thrust faults (TF), filled symbols. Lines of constant slope are shown: $n = 1$, dotted, with $D/L = \gamma$.

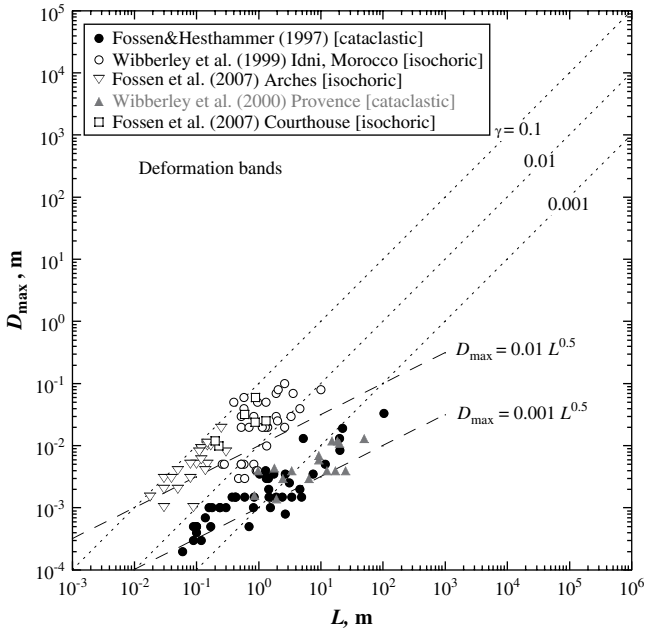

Fig. 3. Compilation of deformation bands; see Fossen and Hesthammer (1997), Fossen et al. (2007), and the Appendix for sources of data and discussion. Cataclastic bands, filled circles and triangles; isochoric shear bands, open symbols. Lines as in Fig. 2.

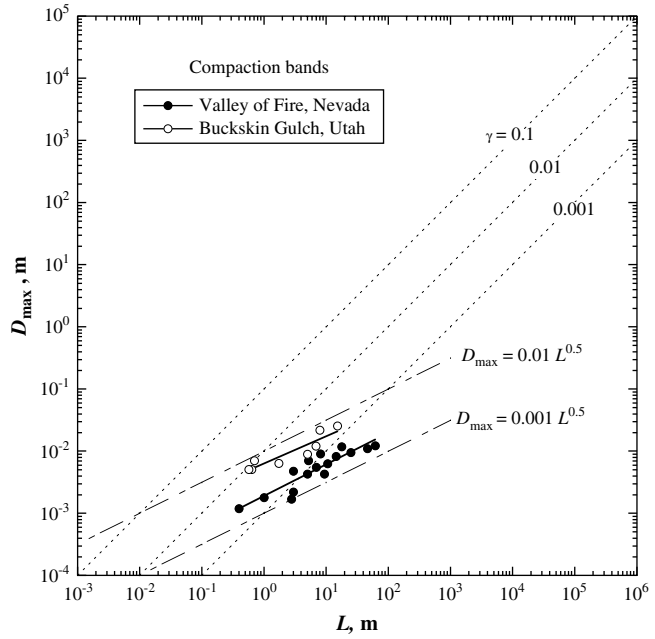

Fig. 4. Compilation of compaction bands; see Sternlof et al. (2005), Schultz (in press), and the Appendix for sources of data and discussion. Lines as in Fig. 2.

from both field sites define a scaling exponent, with differing values of the proportionality constant α, of approximately $n = 0.5$ (Fig. 4).

3. Physical interpretation of the slopes

The scaling relations of geologic structural discontinuities appear to define two separate groups (Fig. 5). The first group, having a power-law slope of approximately $n = 1$ and therefore a linear dependence of maximum displacement and discontinuity length ($D_{max} = \gamma L$), comprises faults and shear deformation bands. The second group, having a power-law slope of approximately $n = 0.5$ and therefore a square root dependence of maximum displacement and discontinuity length ($D_{max} = \alpha L^{0.5}$), comprises joints, veins, igneous dikes, cataclastic (compactional shear) deformation bands, and compaction bands, all of which accommodate significant changes in volume across them. In the following sections we explore the mechanics of these structures in relation to their displacement–length scaling characteristics.

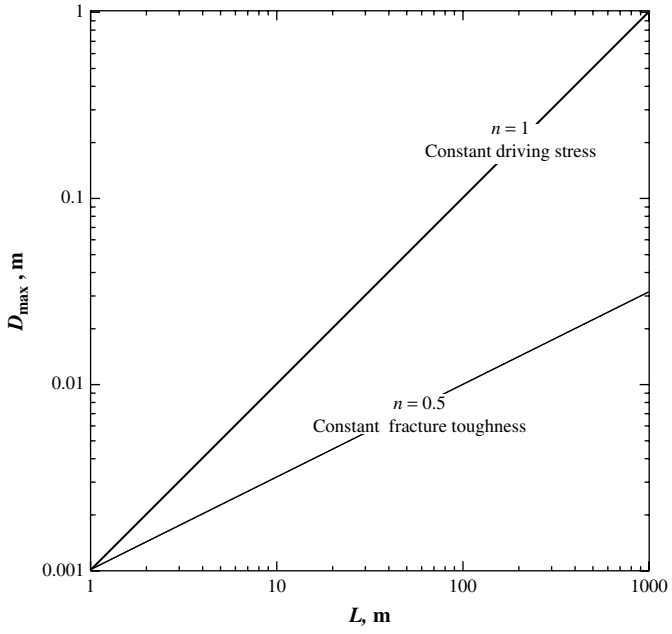

Fig. 5. Theoretical slopes of displacement–length scaling relations for geologic structural discontinuities that accommodate either predominantly shear or volumetric displacements.

3.1. Faults

Linear displacement–length scaling ($n = 1.0$) for normal, strike-slip, and thrust faults is well documented from numerous studies in the literature (e.g. Cowie and Scholz, 1992a; Clark and Cox, 1996; Schlische et al., 1996; Xu et al., 2005; Schultz et al., 2006). The physical explanation for this scaling relation involves elimination of the theoretical stress singularity at a fault tip by allowing for either multiple slip events (Cowie and Shipton, 1998) or a reduction in frictional resistance (Bürgmann et al., 1994; Cooke, 1997; Martel, 1997) along the fault; implicit in the scaling is the predominance of shearing strain over volumetric strain across the faults. Both of these effects (i.e. elimination of the stress singularity, non-constant stress drop) reduce the displacement gradient along the fault (e.g. Cowie and Scholz, 1992b; Bürgmann et al., 1994; Manighetti et al., 2001, 2005; Scholz and Lawler, 2004) below the ideal elliptical one associated with Linear Elastic Fracture Mechanics (LEFM) models of faults (e.g. Pollard and Segall, 1987) and remove the dependence of fault propagation on the rock's opening-mode or shearing-mode fracture toughnesses (K_{Ic}, K_{IIc}, K_{IIIc}; e.g. Cowie and Scholz, 1992b; Bürgmann et al., 1994).

Displacement–length scaling relations for faults can be described by (Scholz, 1997; Schultz et al., 2006)

$$\frac{D_{max}}{L} = \frac{2(1-\nu^2)}{E} N(\sigma_d - C\sigma_y) \quad (1)$$

in which D_{max} is the (maximum) shearing displacement located at or near the fault midpoint, L is horizontal fault length, σ_d is the shear driving stress (Cowie and Scholz, 1992b; Gupta and Scholz, 2000; Schultz, 2003), σ_y is the yield strength of rock at the fault tip, E and ν are Young's modulus and Poisson's ratio of the surrounding rock, N is the ratio of geologic offset to short-term slip, and C is a variable or function that specifies how the theoretical stress singularity at the fault tip is removed (Bürgmann et al., 1994; Schultz et al., 2006). The D_{max}/L ratio depends explicitly and linearly on the driving stress (which is independent of fault length), rock properties, and yield strength. This class of models provides a physical basis for displacement–length scaling relations of the form $D_{max}/L = \gamma$ (e.g. Cowie and Scholz, 1992b; Scholz, 1997, 2002), with γ being equal to the right-hand side of Eq. (1). Because Eq. (1) does not contain a term for the rock's fracture toughness, fault propagation occurs when the yield strength σ_y is exceeded at the fault tip (e.g. Bürgmann et al., 1994; Scholz and Lawler, 2004).

As demonstrated in seismological studies of earthquake faults, the stress drop (or shear driving stress) is relatively constant on faults in a wide range of rock types and tectonic settings (e.g. Scholz, 2002, p. 205), implying that these structures accumulate offsets and propagate under conditions of approximately constant (shear) driving stress (e.g. Cowie and Scholz, 1992b; Scholz, 1997). In particular, the shear driving stress acting on faults is related to the difference between the maximum ("static") friction μ_0 and the long-term, steady-state value μ_{ss} (with $\mu_0 > \mu_{ss}$; Marone, 1998; Paterson and Wong, 2005, p. 261) times a constant N on the order of 10^3 that scales individual slip events to cumulative geologic offset along the fault (Schultz et al., 2006; Cowie and Scholz, 1992b). Values of maximum friction coefficient are in the range of 0.2–0.8 (e.g. Paterson and Wong, 2005, p. 167). The steady-state friction

value represents the residual frictional strength of a fault that is achieved over large displacements (e.g. near a fault's midpoint) and times, independent of the choice of rate-and-state formulations (Marone, 1998; Paterson and Wong, 2005, p. 261). Values of steady-state friction depend on the time-dependence of friction and its evolution with sliding velocity and post-slip healing (e.g. Marone, 1998). Because fault interaction changes the magnitude of normal and shear stresses on closely spaced faults, corresponding fluctuations in the shear driving stress due to fault interaction will modify the value of D_{max} for a given fault or fault segment in a population.

3.2. Joints, veins, and dikes

The data compiled in Fig. 2 for geologic structural discontinuities of opening-mode type (mode-I in fracture mechanics; Broek, 1986) are consistent with scaling according to the power-law relation $D_{max} = \alpha L^n$, with an exponent $n = 0.5$, rather than $D_{max} = \gamma L^n$, with $n = 1.0$, characteristic of sliding- (or tearing-) mode discontinuities such as faults. This $\sqrt{L}$ scaling relation is evident for isolated joints in sandstone outcrops (Moros, 1999, and Appendix) that are not significantly influenced by the mechanical stratigraphy. Similarly, the field observations and data from the Lodève basin sparitic sinuous vein set (de Jossineau et al., 2005) reveal a broadly constant fracture aspect ratio (horizontal length L/vertical, down-dip height H) of 2 over the range of fracture lengths, consistent with the veins not being stratigraphically restricted (Petit et al., 1994). A second data set for igneous dikes in basaltic host rock that was recently reported by Schultz et al. (in press) (see Appendix) also exhibits a scaling exponent of ~0.5 over the range of dike lengths. These data sets, characterized by scaling exponents of $n = 0.5$, can be analyzed by assuming that they approximate LEFM conditions in the sense that their dimensions, scaling, and growth are regulated by the near-tip fracture toughness of the host rock (Olson, 2003); i.e.,

$$D_{max} = \frac{K_c(1-\nu^2)}{E}\frac{\sqrt{8}}{\sqrt{\pi}}\sqrt{L} \quad (2)$$

in which K_c is the fracture toughness, ν is Poisson's ratio, and E is Young's modulus (all of the host rock). Following Olson (2003), his Eq. (6), values of (opening-mode or closing-mode) fracture toughness for a given fracture population can be obtained by using the measured lengths L and maximum (opening or closing) displacements D_{max} from a data set in Eq. (2) and solving for K_c. As a result, if values of rock stiffness (modulus and Poisson's ratio) are known, then the rock's opening- or closing-mode fracture toughness can be obtained from the scaling relations.

3.3. Deformation bands

The scaling of cataclastic compactional shear deformation bands was recently discussed by Fossen et al. (2007) who noted that both the host rock's fracture toughness and the confining effect of stratigraphy may influence the scaling parameters. For both data sets of cataclastic compactional shear bands evaluated (Fig. 3), a scaling exponent of approximately $n = 0.5$ is consistent with the data. A population of nearly isochoric (disaggregation or "invisible") shear deformation bands (see Appendix) was also reported in that work which is shown in this paper to be consistent with $n = 1$ scaling (Fig. 3). These bands lack significant volumetric normal strains across them, as evidenced by the lack of increased porosity (leading to dilational or opening-mode displacements) or decreased porosity (contractional or anticrack displacements); instead, only shear strains are accommodated across the bands. In this sense, isochoric shear bands are analogous mechanically to faults and slip surfaces, all of which accommodate predominately shear displacements (e.g. Pollard and Segall, 1987; Aydin and Schultz, 1990).

In-plane propagation of shear bands in the mode-II direction (i.e. parallel to the direction of shearing) is well known in soils (e.g. Wolf et al., 2003), unconsolidated sands (e.g. Saada et al., 1999), and in materials such as wet plaster (Fossen and Gabrielsen, 1996) although it is not associated with mode-II propagation of faults under LEFM (e.g. Pollard and Segall, 1987; Willemse and Pollard, 1998) and peak-strength (Du and Aydin, 1993, 1995) conditions. The in-plane propagation of shear bands and cataclastic compactional shear deformation bands has been understood by calculating the distortional strain-energy density at the band tip (Schultz and Balasko, 2003; Okubo and Schultz, 2005, 2006). Propagation occurs when the shear yield strength is exceeded by amplified stresses near the band tip (Schultz and Balasko, 2003).

Recent work shows that cataclastic compactional shear deformation bands first strain soften as a result of grain cracking as they shear, leading to an initially reduced stiffness (Young's or shear modulus) within the band (Katsman et al., 2004, 2006; Katsman and Aharonov, 2006) and attendant increase in porosity within it. As shear strain within the band increases, the newly angular fractured grains interlock, leading to increased frictional strength and attendant strain hardening within the band (Mair et al., 2002). Shear strains accumulate while cataclasis and flow occur within the band, so in-plane propagation of cataclastic compactional shear bands (and compactional shear bands that lack cataclasis; Antonellini et al., 1994) likely occurs during shear strain accumulation before the band strain hardens significantly. However, the relative magnitudes of shear and normal strain in compactional shear bands are difficult to quantify in natural examples (Aydin et al., 2006). Because cataclasis is controlled at the grain scale by the mode-I fracture toughness (Zhang et al., 1990), a smaller scaling exponent than $n = 1$ may be associated with deformation bands having a sufficiently large component of normal (opening or closing) strain across them, or during that part of their history when grain cracking was important, for their propagation to be limited by the ability of near-tip stress to crack grains (see also the discussion by Wang et al., 2008).

3.4. Compaction bands

Recent work by Sternlof et al. (2005) and Rudnicki and Sternlof (2005) demonstrated that compaction bands in the Valley of Fire area of southern Nevada are consistent with LEFM assumptions, including nearly constant contractional normal strain across them (implying constant driving stress along the bands), negligibly small near-tip process zones, and elliptical thickness (contractional displacement) profiles along the bands. As a result, scaling with an exponent of $n = 0.5$ (Fig. 4) is perhaps not surprising for these structures (see parallel conclusions reported previously by Rudnicki, 2007), consistent with observations of grain cracking along the bands and at band tips.

The population exponent of $n = 0.5$ is consistent with compaction band propagation being controlled by the tensile strength of grains within a small volume around the tips of the bands, as discussed at length by Wang et al. (2008) in analogy, for example, with failure in tension of a disc loaded in compression during a Brazilian strength text (e.g. Broch and Franklin, 1972). This result parallels the dependence of the critical pressure for grain cracking and cataclasis for compactional shear bands and compaction bands on the host rock fracture toughness as noted by Zhang et al. (1990), Wong et al. (2004), and Wang et al. (2008).

The approach of Olson (2003), as used in this paper, can provide estimates of the near-tip properties of the host rock during compaction band propagation. Using values of length and maximum thickness (related to the compactional normal strain

across a band by Rudnicki, 2007; Holcomb et al., 2007; Tembe et al., in press) from the compaction band data set of Sternlof et al. (2005) in Eq. (2) with values of Young's modulus and Poisson's ratio of 20 GPa and 0.2, respectively, for Aztec Sandstone (Rudnicki and Sternlof, 2005), the host rock fracture toughness is calculated here from the band population statistics to be $K_c = 18 - 34$ MPa m$^{1/2}$. Using the standard plane-strain conversion (assuming LEFM conditions; e.g. Broek, 1986) to strain-energy release rate $G = (K_c)^2(1-\nu^2)/E$, this value becomes $G = 14 - 60$ kJ/m^2, in excellent agreement with the values of $G = 10$–60 kJ/m^2 calculated independently by using the J-integral approach by Rudnicki and Sternlof (2005).

Measurements of compaction bands at the Buckskin Gulch site of southern Utah (Mollema and Antonellini, 1996) obtained by Schultz (in press) also indicate scaling of these bands as $D_{max} \propto \sqrt{L}$ (Fig. 4; see description of data in the Appendix). Using the same values of E and ν from the Nevada bands gives a value of $K = 60 - 100$ kJ/m^2 for the Utah bands, a value that is about a factor of 3 larger than for bands at the Nevada site despite the host rocks at both sites being correlative and similar in grain size and porosity. Rudnicki (2007) showed that the stress intensity factor for a compaction band having a flattened displacement profile is increased relative to that for a band having an elliptical (non-flattened) displacement profile, although no physical mechanism was suggested to account for profile flattening in his work. Interestingly, compaction bands at the Utah site show flattened displacement profiles (Schultz, in press). Reducing K by a factor of about 3 to account for an increased stress intensity factor associated with flattened displacement profiles along the compaction bands at the Utah site over the full range of band lengths leads to $K_c = 20 - 34$ MPa m$^{1/2}$ (Schultz, in press), which is consistent with the values obtained for bands from the Nevada site by Rudnicki and Sternlof (2005).

4. Discussion and implications

Scaling of opening- and closing-mode structures with $n \sim 0.5$ appears to be evident for joints, veins, igneous dikes, cataclastic compactional shear deformation bands, and compaction bands, suggesting that the opening-mode or closing-mode fracture toughness K_c controls their propagation and hence their length and maximum displacement values. Displacement–length data for other joint and vein sets, however, are not well described by $n = 0.5$. For example, the measurements of joints in outcrop having varying degrees of interaction and linkage show exponents between 0.5 and 1.0 with wide scatter (e.g. Hatton et al., 1994; Moros, 1999). Mechanical interaction between joints and veins transfers displacement between them, resulting in different values of opening displacement depending on the position of the fracture within an array (e.g. Olson, 2003). Additionally, echelon sigmoidal veins growing within a shear zone (e.g. Olson and Pollard, 1991; Johnston and McCaffrey, 1996) likely scale differently than would spatially isolated veins, having pure opening displacements, in the same rock. Increases in exponent values above $n = 0.5$ can also arise from post-propagation conditions (e.g. Olson, 2003). Vein and dike apertures may not be relaxed significantly following propagation, whereas joint apertures are void spaces subject to perturbations in the local stress state that can lead to relaxation and further dilation of the joints without propagation. Since D–L data on spatially isolated joints are typically collected from outcrops or exposures at the surface, changes in the local stress state there could promote additional joint dilation, and hence, higher exponent values than $n = 0.5$ with increased scatter in the data.

Restriction of the vertical extent of geologic structural discontinuities by stratigraphy (Nicol et al., 1996; Wilkins and Gross, 2002; Benedicto et al., 2003) is clearly recognized in displacement–length data for certain fault sets (e.g. Soliva et al., 2005), and other attributes such as perpendicular spacing, and relay-ramp dimensions (Soliva and Benedicto, 2004, 2005; Soliva et al., 2006) are physically related to fault restriction, and thus to the minimum fault dimension (i.e. height H rather than length L). However, the influence of stratigraphic restriction on the scaling relations for structures other than faults, such as joints or bands, remains less clear. For example, as a layer extends due to remote displacement loading (such as bending), unstable propagation of joints may initially occur (Segall, 1984; Olson, 2003), scaling approximately as $n = 1.0$, followed by stable propagation with an implied decrease in scaling exponent (Olson, 2003). Interestingly, the cataclastic compactional shear deformation bands measured by Fossen and Hesthammer (1997) show a steeper slope at the smaller lengths of approximately $n = 1.0$ and a shallower slope of approximately $n = 0.5$ at longer lengths (Fig. 3, filled circles). At present, however, it is unclear how these scenarios apply in detail to either joints or deformation bands growing within a layer of given thickness given the wide variability in joint measurements and network properties (e.g. Olson, 2007) and the sparseness of available displacement–length data for deformation (and compaction) bands. Detailed measurements of joint and band displacements and microstructural observations over a range of lengths may help to resolve the possible relationships between of scaling changes and restriction for these structures.

Following Clark and Cox (1996), displacement–length scaling relations (and a single power-law fit) are applicable to individual data sets only, rather than to a compiled data set containing structures in different rock types (Cowie and Scholz, 1992a). This is due, in part, because variations in modulus or fracture toughness of the host rock contribute to vertical shifts in position of the data on the displacement–length diagram (e.g. Cowie and Scholz, 1992b; Olson, 2003; Gudmundsson, 2004; Schultz et al., 2006), leading to poorer fits and different slopes than would be appropriate to the individual data sets themselves. Mechanism-dependent variations in the scaling relations may also be more clearly revealed by analysis of the individual data sets (e.g. Hatton et al., 1994; Wilkins and Gross, 2002; Crider and Peacock, 2004). As more data sets become available, for example for compaction bands (Holcomb et al., 2007; Schultz, in press), power-law fits should be made for individual data sets and not for the compiled suite, as emphasized by Clark and Cox (1996), in order to more clearly reveal slopes and intercepts associated with near-tip and host rock properties.

5. Conclusions

Geologic structural discontinuities that accommodate predominantly shear strain across them, such as faults and shear deformation bands, exhibit linear displacement–scaling relations, with $n = 1.0$ and an intercept γ that is related to host rock stiffness (Young's modulus, Poisson's ratio) and driving stress. The power-law scaling exponent changes to $n = 0.5$ for geologic structural discontinuities that accommodate significant volumetric changes, such as opening (joints, veins, dikes) or closing (compactional shear deformation bands, compaction bands) strains across them. In this second case, the intercept α contains information on rock stiffness and the fracture toughness that regulated propagation. Volumetric changes in the deforming rock, at the tip of the structural discontinuity, are therefore systematically associated with the scaling exponent, revealing that the processes related to propagation and displacement accumulation are significantly different for structures that accommodate shear or volumetric strains.

Opening and closing structures having power-law scaling exponents of $n = 0.5$ approximate LEFM conditions such as small-scale yielding and concomitant large stress concentration at the tip, nearly elliptical displacement profiles, and propagation under

conditions of constant rock fracture toughness. Shear-dominated structures, on the other hand, that grow under conditions of constant driving stress exhibit larger-scale near-tip deformation and, therefore, growth under non-LEFM conditions. The results presented in this paper are important for brittle strain calculations or estimates of fracture densities in different lithologies and structural contexts given the sensitivity of these quantities to the displacement–length scaling relations.

Acknowledgments

We thank Randy Marrett for providing data for joints from Javier Moros' M.S. thesis, Jan Vermilye for a copy of her dissertation, and Sheryl Tembe for a preprint of her work on compaction bands. Thanks to John Rudnicki for a preprint of his 2007 paper and for discussions on compaction band mechanics. Detailed and thoughtful reviews by Nancye Dawers and an anonymous referee improved the clarity and exposition of the paper. This work was supported by grants from NASA's Planetary Geology and Geophysics Program and the Mars Data Analysis Program to RAS.

Appendix

Careful measurements of joint aperture and length were reported by Moros (1999) for joints in two sandstone outcrops. The joint data shown in Fig. 2 were extracted from his Table 5 by selecting only joints in sandstone outcrop that were listed as isolated; this excluded interacting or linked structures and those he measured in thin section and in core. Outcrop data were taken from the Hickory Sandstone (Cambrian Riley Formation) in central Texas, with a thickness of ~160 m. Joints measured by Moros (1999) in Marble Falls Limestone were members of echelon arrays and so were not included in Fig. 2.

A new data set of 39 igneous (basaltic and silicic) dikes from the Ethio-Sudanese plain, west of the Abyssinian volcanic plateau in northwest Ethiopia was reported and analyzed by Schultz et al. (in press). The dikes cut a 30–31 Ma ~100-m-thick basalt sequence (the Trap Series) that overlies Precambrian basement. The dikes were initially described by Mège and Korme (2004a) and their length–frequency statistics were analyzed by Mège and Korme (2004b).

Only two D–L data sets from disaggregation bands are currently known to us. One was published by Wibberley et al. (1999) and is from bedding-plane observations of Triassic sandstones in the Idni area, Morocco, formed prior to lithification at 200–500 m depth. Another was collected in Arches National Park, Utah in the vicinity of the Moab Fault (reported by Fossen et al., 2007). The Utah bands occur in fine-grained eolian Navajo Sandstone and appear to be associated with soft-sediment deformation (folding) of dune structures prior to deposition of the directly overlying Dewey Bridge Member. The Arches disaggregation bands are almost completely invisible except where lamination is present and offset in the sandstone, and appear to primarily accommodate shearing strains. They are overprinted by the cataclastic deformation bands described by Antonellini et al. (1994). The measurements presented in Fig. 3 were obtained on surfaces where laminae more resistant to weathering exhibit the displacement variations along the bands.

Data from a population of small slip surfaces in the lower fluvial sandstone layer of the Tidwell Member of the Jurassic Morrison Formation, a relatively low-porosity sandstone in the Courthouse Rock area of Utah, are also plotted in Fig. 3. These slip surfaces formed in fluvial sandstone layers between the Moab Fault and the Courthouse Fault near their branch point. Slip surfaces are thought to have formed in this sandstone rather than deformation bands due to the low porosity of the Tidwell Member sandstones in this area. This is further related to quartz dissolution and cementation prior to faulting, as discussed in Johansen et al. (2005).

Measurements of compaction bands from the Buckskin Gulch site in southern Utah (Mollema and Antonellini, 1996), reported by Schultz (in press), were taken from eight bands having clear terminations and minimal geometric complexities with nearby bands. Thickness was measured as a proxy for the magnitude of closing displacement along a band, following Sternlof et al. (2005) and Holcomb et al. (2007), an approach supported on theoretical grounds by Rudnicki (2007) and Tembe et al. (in press) by relating band thickness to closing displacement through the degree of porosity reduction (~20%) within the band. Band lengths, measured by using a steel tape, ranged from 0.57 to 15.3 m, with thicknesses, measured by using a caliper, having maximum values between 5.1 and 25.4 mm; thickness and length have measurement uncertainties of ±0.2 mm and ±1 mm, respectively. Displacement–length scaling relations for the compaction bands were obtained from these values of length L and maximum thickness, here called the maximum displacement, D_{max}, for consistency with the other structures analyzed in this paper.

References

Antonellini, M., Aydin, A., Pollard, D.D., 1994. Microstructure of deformation bands in porous sandstones at Arches National Park, Utah. Journal of Structural Geology 16, 941–959.
Aydin, A., Borja, R.I., Eichhubl, P., 2006. Geological and mathematical framework for failure modes in granular rock. Journal of Structural Geology 28, 83–98.
Aydin, A., Schultz, R.A., 1990. Effect of mechanical interaction on the development of strike-slip faults with echelon patterns. Journal of Structural Geology 12, 123–129.
Benedicto, A., Schultz, R., Soliva, R., 2003. Layer thickness and the shape of faults. Geophysical Research Letters 30, 2076, doi:10.1029/2003GL018237.
Broch, E., Franklin, J.A., 1972. The point-load strength test. International Journal of Rock Mechanics and Mining Sciences 9, 669–697.
Broek, D., 1986. Elementary Engineering Fracture Mechanics, fourth ed. Martinus Nijhoff, Boston.
Bürgmann, R., Pollard, D.D., Martel, S.J., 1994. Slip distributions on faults: effects of stress gradients, inelastic deformation, heterogeneous host-rock stiffness, and fault interaction. Journal of Structural Geology 16, 1675–1690.
Clark, R.M., Cox, S.J.D., 1996. A modern regression approach to determining fault displacement–length relationships. Journal of Structural Geology 18, 147–152.
Cooke, M.L., 1997. Fracture localization along faults with spatially varying friction. Journal of Geophysical Research 102, 22425–22434.
Cowie, P.A., Scholz, C.H., 1992a. Displacement–length scaling relationships for faults: data synthesis and discussion. Journal of Structural Geology 14, 1149–1156.
Cowie, P.A., Scholz, C.H., 1992b. Physical explanation for the displacement–length relationship of faults using a post-yield fracture mechanics model. Journal of Structural Geology 14, 1133–1148.
Cowie, P.A., Shipton, Z.K., 1998. Fault tip displacement gradients and process zone dimensions. Journal of Structural Geology 20, 983–997.
Crider, J.A., Peacock, D.C.P., 2004. Initiation of brittle faults in the upper crust: a review of field observations. Journal of Structural Geology 26, 691–707.
Du, Y., Aydin, A., 1993. The maximum distortional strain energy density criterion for shear fracture propagation with applications to the growth paths of *en échelon* faults. Geophysical Research Letters 20, 1091–1094.
Du, Y., Aydin, A., 1995. Shear fracture patterns and connectivity at geometric complexities along strike-slip faults. Journal of Geophysical Research 100, 18093–18102.
Fossen, H., Gabrielsen, R.H., 1996. Experimental modeling of extensional fault systems by use of plaster. Journal of Structural Geology 18, 673–687.
Fossen, H., Hesthammer, J., 1997. Geometric analysis and scaling relations of deformation bands in porous sandstone. Journal of Structural Geology 19, 1479–1493.
Fossen, H., Schultz, R.A., Shipton, Z.K., Mair, K., 2007. Deformation bands in sandstone: a review. Journal of the Geological Society of London 164, 755–769.
Gudmundsson, A., 2004. Effects of Young's modulus on fault displacement. Comptes Rendus Geosciences 336, 85–92.
Gupta, A., Scholz, C.H., 2000. A model of normal fault interaction based on observations and theory. Journal of Structural Geology 22, 865–879.
Hatton, C.G., Main, I.G., Meredith, P.G., 1994. Non-universal scaling of fracture length and opening displacement. Nature 367, 160–162.
Holcomb, D., Rudnicki, J.W., Issen, K.A., Sternlof, K., 2007. Compaction localization in the earth and the laboratory: state of the research and research directions. Acta Geotechnica 2, 1–15.
de Jossineau, G., Bazalgette, L., Petit, J.-P., Lopez, M., 2005. Morphology, intersections, and syn/late-diagenetic origin of vein networks in pelites of

the Lodève Permian Basin, Southern France. Journal of Structural Geology 27, 67–87.
Johansen, T.E.S., Fossen, H., Kluge, R., 2005. The impact of syn-kinematic porosity reduction on damage zone architecture in porous sandstone; an outcrop example from the Moab Fault, Utah. Journal of Structural Geology 27, 1469–1485.
Johnston, J.D., McCaffrey, K.J.W., 1996. Fractal geometries of vein systems and the variation of scaling relationships with mechanism. Journal of Structural Geology 18, 349–358.
Katsman, R., Aharonov, E., Scher, H., 2004. Numerical simulation of compaction bands in high-porosity sedimentary rock. Mechanics of Materials 37, 371–390.
Katsman, R., Aharonov, E., 2006. A study of compaction bands originating from cracks, notches and compacted defects. Journal of Structural Geology 28, 508–518.
Katsman, R., Aharonov, E., Scher, H., 2006. Localized compaction in rocks: Eshelby's inclusion and the spring network model. Geophysical Research Letters 33, L10311, doi:10.1029/2005GL025628.
Mair, K., Frye, K.M., Marone, C., 2002. Influence of grain characteristics on the friction of granular shear zones. Journal of Geophysical Research 107, 2219, doi:10.1029/2001JB000516.
Manighetti, I., King, G.C.P., Gaudemer, Y., Scholz, C.H., Doubre, C., 2001. Slip accumulation and lateral propagation of active normal faults in Afar. Journal of Geophysical Research 106, 13667–13696.
Manighetti, I., Campillo, M., Sammis, C., Mai, P.M., King, G., 2005. Evidence for self-similar, triangular slip distributions on earthquakes: implications for earthquake and fault mechanics. Journal of Geophysical Research 110, B05302, doi:10.1029/2004JB003174.
Marone, C., 1998. Laboratory-derived friction laws and their application to seismic faulting. Annual Review of Earth and Planetary Sciences 26, 643–696.
Martel, S.J., 1997. Effects of cohesive zones on small faults and implications for secondary fracturing and fault trace geometry. Journal of Structural Geology 19, 835–847.
Mège, D., Korme, T., 2004a. Dyke swarm emplacement in the Ethiopian large igneous province: not only a matter of stress. Journal of Volcanology and Geothermal Research 132, 283–310.
Mège, D., Korme, T., 2004b. Fissure eruption of flood basalts from statistical analysis of dyke fracture length. Journal of Volcanology and Geothermal Research 131, 77–92.
Mollema, P.N., Antonellini, M.A., 1996. Compaction bands: a structural analog for anti-mode I cracks in aeolian sandstone. Tectonophysics 267, 209–228.
Moros, J.G., 1999. Relationship between fracture aperture and length in sedimentary rocks. Unpublished M.S. thesis. The University of Texas, Austin.
Nicol, A., Watterson, J., Walsh, J.J., Childs, C., 1996. The shapes, major axis orientations and displacement patterns of fault surfaces. Journal of Structural Geology 18, 235–248.
Okubo, C.H., Schultz, R.A., 2005. Evolution of damage zone geometry and intensity in porous sandstone: insight from strain energy density. Journal of the Geological Society of London 162, 939–949.
Okubo, C.H., Schultz, R.A., 2006. Near-tip stress rotation and the development of deformation band stepover geometries in mode II. Geological Society of America Bulletin 118, 343–348.
Olson, J.E., 2003. Sublinear scaling of fracture aperture versus length: an exception or the rule? Journal of Geophysical Research 108, 2413, doi:10.1029/2001JB000419.
Olson, J.E., 2007. Fracture aperture, length and pattern geometry development under biaxial loading: a numerical study with applications to natural, cross-jointed systems. In: Couples, G., Lewis, H. (Eds.), Fracture-like Damage and Localisation. Geological Society, London, Special Publication, vol. 289, pp. 123–142.
Olson, J.E., Pollard, D.D., 1991. The initiation and growth of en échelon veins. Journal of Structural Geology 13, 595–608.
Paterson, M.S., Wong, T.-F., 2005. Experimental Rock Deformation – the Brittle Field, second ed. Springer-Verlag, Heidelberg.
Petit, J.-P., Massonnat, G., Pueo, F., Rawnsley, K., 1994. Mode 1 fracture shape ratios in layered rocks: a case study in the Lodève Permian Basin (France). In: Bulletin des Centres de Recherches Exploration-Production, Elf Aquitane, vol. 18, pp. 211–229.
Pollard, D.D., Segall, P., 1987. Theoretical displacements and stresses near fractures in rock: with applications to faults, joints, veins, dikes, and solution surfaces. In: Atkinson, B.K. (Ed.), Fracture Mechanics of Rock. Academic Press, London, pp. 277–349.
Rudnicki, J.W., 2007. Models for compaction band propagation. In: David, C., Le Ravalec-Dupin, M. (Eds.), Rock Physics and Geomechanics in the Study of Reservoirs and Repositories. Geological Society, London, Special Publication, vol. 284, pp. 107–125.
Rudnicki, J.W., Sternlof, K.R., 2005. Energy release model of compaction band propagation. Geophysical Research Letters 32, L16303, doi:10.1029/2005GL023602.
Saada, A.S., Liang, L., Figueroa, J.L., Cope, C.T., 1999. Bifurcation and shear band propagation in sands. Géotechnique 49, 367–385.
Schlische, R.W., Young, S.S., Ackermann, R.V., Gupta, A., 1996. Geometry and scaling relations of a population of very small rift related normal faults. Geology 24, 683–686.
Scholz, C.H., 1997. Earthquake and fault populations and the calculation of brittle strain. Geowissenschaften 15, 124–130.
Scholz, C.H., 2002. The Mechanics of Earthquakes and Faulting, second ed. Cambridge University Press, 471 pp.
Scholz, C.H., Lawler, T.M., 2004. Slip tapers at the tips of faults and earthquake ruptures. Geophysical Research Letters 31, L21609, doi:10.1029/2004GL021030.
Schultz, R.A., 1999. Understanding the process of faulting: selected challenges and opportunities at the edge of the 21st century. Journal of Structural Geology 21, 985–993.
Schultz, R.A., 2003. A method to relate initial elastic stress to fault population strains. Geophysical Research Letters 30, 1593, doi:10.1029/2002GL016681.
Schultz, R.A. Scaling and paleodepth of compaction bands. Journal of Geophysical Research, in press.
Schultz, R.A., Balasko, C.M., 2003. Growth of deformation bands into echelon and ladder geometries. Geophysical Research Letters 30, 2033, doi:10.1029/2003GL018449.
Schultz, R.A., Fossen, H., 2002. Displacement–length scaling in three dimensions: the importance of aspect ratio and application to deformation bands. Journal of Structural Geology 24, 1389–1411.
Schultz, R.A., Fossen, H., 2008. Terminology for structural discontinuities. American Association of Petroleum Geologists Bulletin 92, 853–867.
Schultz, R.A., Mège, D., Diot, H., Emplacement conditions of igneous dikes in Ethiopian traps. Journal of Volcanology and Geothermal Research, in press.
Schultz, R.A., Siddharthan, R., 2005. A general framework for the occurrence and faulting of deformation bands in porous granular rocks. Tectonophysics 411, 1–18.
Schultz, R.A., Okubo, C.H., Wilkins, S.J., 2006. Displacement–length scaling relations for faults on the terrestrial planets. Journal of Structural Geology 28, 2182–2193.
Segall, P., 1984. Formation and growth of extensional fracture sets. Geological Society of America Bulletin 95, 454–462.
Soliva, R., Benedicto, A., 2004. A linkage criterion for segmented normal faults. Journal of Structural Geology 26, 2251–2267.
Soliva, R., Benedicto, A., 2005. Geometry, scaling relation and spacing of vertically restricted normal faults. Journal of Structural Geology 27, 317–325.
Soliva, R., Benedicto, A., Maerten, L., 2006. Spacing and linkage of confined normal faults: importance of mechanical thickness. Journal of Geophysical Research 111, B01402, doi:10.1029/2004JB003507.
Soliva, R., Schultz, R.A., Benedicto, A., 2005. Three-dimensional displacement–length scaling and maximum dimension of normal faults in layered rocks. Geophysical Research Letters 32, L16302, doi:10.1029/2005GL023007.
Sternlof, K.R., Rudnicki, J.W., Pollard, D.D., 2005. Anticrack inclusion model for compaction bands in sandstone. Journal of Geophysical Research 110, B11403, doi:10.1029/2005JB003764.
Tembe, S., Baud, P., Wong, T.-F. Stress conditions for the propagation of discrete compaction bands in porous sandstone. Journal of Geophysical Research 113, in press, doi:10.1029/2007JB005439.
Vermilye, J.M., Scholz, C.H., 1995. Relation between vein length and aperture. Journal of Structural Geology 17, 423–434.
Wang, B., Chen, Y., Wong, T.-F., 2008. A discrete element model for the development of compaction localization in granular rock. Journal of Geophysical Research 113, B03202, doi:10.1029/2006JB004501.
Wibberley, C.A.J., Petit, J.-P., Rives, T., 1999. Mechanics of high displacement gradient faulting prior to lithification. Journal of Structural Geology 21, 251–257.
Wibberley, C.A.J., Petit, J.-P., Rives, T., 2000. Mechanics of cataclastic 'deformation band' faulting in high-porosity sandstone, Provence. Earth and Planetary Sciences 331, 419–425.
Wilkins, S.J., Gross, M.R., 2002. Normal fault growth in layered rocks at Split Mountain, Utah: influence of mechanical stratigraphy on dip linkage, fault restriction and fault scaling. Journal of Structural Geology 24, 1413–1429 (erratum, Journal of Structural Geology 24, 2007).
Willemse, E.J.M., Pollard, D.D., 1998. On the orientation and pattern of wing cracks and solution surfaces at the tips of a sliding flaw or fault. Journal of Geophysical Research 103, 2427–2438.
Willemse, E.J.M., Pollard, D.D., Aydin, A., 1996. Three-dimensional analyses of slip distributions on normal fault arrays with consequences for fault scaling. Journal of Structural Geology 18, 295–309.
Wolf, H., König, D., Triantafyllidis, T., 2003. Experimental investigation of shear band patterns in granular material. Journal of Structural Geology 25, 1229–1240.
Wong, T.-F., David, C., Menéndez, B., 2004. Mechanical compaction. In: Guéguen, Y., Boutéca, M. (Eds.), Mechanics of Fluid-saturated Rocks. Elsevier, Amsterdam, pp. 55–114.
Xu, S.-S., Nieto-Samaniego, A.F., Alaniz-Álvarez, S.A., Velasquillo-Martínez, L.G., 2005. Effect of sampling and linkage on fault length and length–displacement relationship. International Journal of Earth Sciences 95, 841–853.
Zhang, J., Wong, T.-F., Davis, D.M., 1990. Micromechanics of pressure-induced grain crushing in porous rocks. Journal of Geophysical Research 95, 341–352.